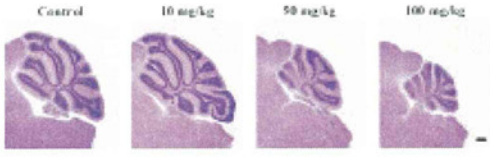

Fig. 2. Changes in the cerebellar size of ptch1 mice receiving *N*-ethyl-*N*-nitrosourea on postnatal day 1. Bar, 500 μm.

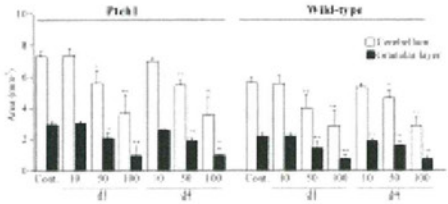

Fig. 3. Areas of the cerebellum and granular layer in ptch1 and wild-type (WT) mice. Significantly different from the control group at $^{*}P < 0.05$ and $^{**}P < 0.01$, respectively. Significantly different from the control group at $^{\dagger\dagger}P < 0.01$.

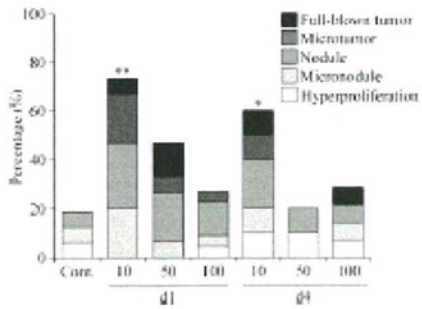

Fig. 4. Total incidence of medulloblastoma in ptch1 mice. Significantly different from the control group at $^{*}P < 0.05$ and $^{**}P < 0.01$, respectively.

zonal distribution parallel to the granular layer in the molecular layer at 100 mg in both ptch1 and WT mice (Fig. 5C,F). The persistent EGL cells of focal and diffuse types were well-differentiated, and cellular atypia and mitosis were rarely seen, unlike in medulloblastoma cells. In accordance with the morphometric analysis, reduction of the number of granule cells was histologically apparent starting at 50 mg. Also, misalignment of Purkinje cells was noted from 50 mg regardless of genotype (Fig. 5D,G).

Other than medulloblastoma, there was no occurrence of neural tumors in ptch1 and WT mice. Thymic lymphoma, which is induced by ENU in mice, was increased dose-dependently. The incidence in ptch1 mice was 14% in the group receiving 100 mg on d1 and 10% and 50% in the groups receiving 50 and 100 mg on d4, respectively. Also in WT mice, thymic lymphoma occurred in 25% and 40% of the d1-treated mice at 50 and 100 mg, respectively, and in 11%, 18% and 67% of the d4-treated mice at 10, 50 and 100 mg, respec-

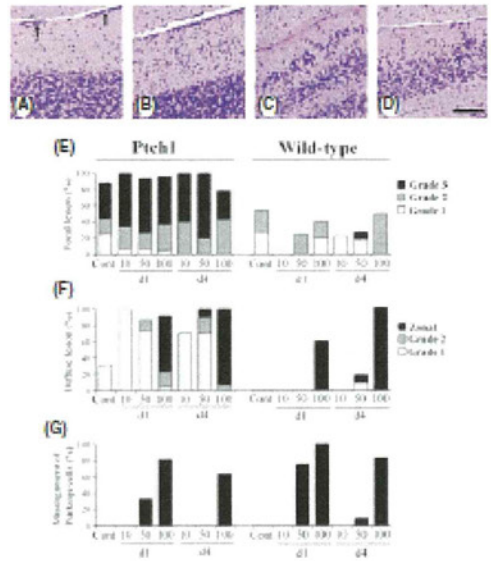

Fig. 5. Histopathological findings observed in cerebellar cortex. Morphologic changes observed in the cerebellar cortex of ptch1 mice, and the incidence of these lesions in ptch1 and wild-type (WT) mice. (A) Focal lesions of persistent external granular layer (EGL) in subpial position (arrows) observed in ptch1 mice of the control group (grade 2). (B) The lesions of persistent EGL cells distributed diffusely in the molecular layer of ptch1 mice receiving 10 mg of *N*-ethyl-*N*-nitrosourea (ENU) on postnatal day 1 (d1) (grade 1). (C) The persistent EGL cells showed zonal distribution parallel to the granular layer in the molecular layer of ptch1 mice receiving 100 mg of ENU on postnatal day 4 (d4). (D) Misalignment of Purkinje cells observed in ptch1 mice receiving 100 mg of ENU on d1. Hematoxylin and eosin section. Bar, 100 μm. The incidence of focal lesions of persistent EGL in subpial position (E), the diffuse lesions of persistent EGL in the molecular layer (F), and misalignment of Purkinje cells (G).

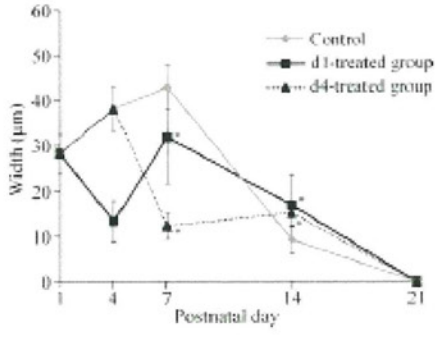

Fig. 6. The width of the external granular layer in the developing cerebellum of mice receiving 100 mg of *N*-ethyl-*N*-nitrosourea on postnatal day 1 (d1) or postnatal day 4 (d4). Significantly different from the control group at $^{*}P < 0.01$.

tively. Hydrocephalus and rhabdomyosarcomas, which are known to occur spontaneously in ptch1 mice, were found in three ptch1 mice each, and ENU did not affect their incidence.

In experiment 2, there were no intergroup differences in body weight throughout the study (data not shown). The width of EGL in the control group peaked at postnatal day 7 and then decreased gradually and disappeared at postnatal day 21 (Fig. 6). In mice receiving 100 mg on d1, the width of EGL was strikingly reduced at d4. Then, EGL considerably recovered at d7 and was wider than the control group at d14. Similarly, the width of EGL in mice of the d4-treated group was significantly decreased at d7 and then became wider than that in the control at d14. But, the degree of recovery after damage by ENU was milder than that in the d1-treated group. Misalignment of Purkinje cells was apparent, especially in the d1-treated group. A difference in EGL development between ptch1 and WT mice was not observed in the present study.

Discussion

Medulloblastomas were observed frequently in 12-week-old ptch1 mice receiving 10 mg of ENU. In ptch1 mice, preneoplastic lesions of medulloblastoma were seen at a high incidence at 2–3 weeks of age, and these lesions spontaneously regressed or matured by 10 weeks of age.[17,18] Therefore, in the present study, the lesions observed at 12 weeks of age were regarded as selected lesions that directly led to tumor, although most lesions were regarded as an early stage of medulloblastoma. It is believed that ptch1 haploinsufficiency alone is not sufficient to induce tumor formation and that additional genetic lesions are required for tumorigenesis.[9,11] Because ENU is a multipotent genotoxic carcinogen, ENU possibly enhanced tumorigenesis by increasing DNA damage similar to radiation and p53 inactivation.[11,19]

As for the dose of ENU, 10 mg appeared to be appropriate for medulloblastoma induction based on the high incidence of medulloblastoma and low impact on cerebellum structure and lymphoma. In contrast, 50 and 100 mg of ENU reduced the size of the cerebellum, and significant induction of medulloblastoma was not observed. In experiment 2, EGL cells, a possible origin of medulloblastoma, were strikingly decreased after 100 mg of ENU. Consequently, the damage of ENU to EGL cells was so severe at a high dose that stockpiles of the damaged EGL cells to develop medulloblastoma could be limited.

Timing of administration is also an important factor for medulloblastoma induction, and in the present study, d1 was more effective than d4. In experiment 2, the response to ENU damage was different between d1 and d4 treatment. The strong recovery of EGL after ENU injection that was observed in the d1-treated group may be a reason for enhanced tumor induction. A previous study demonstrated that EGL cells at d1 showed resistance to radiation-induced cell death and p53 induction compared with EGL cells at d10, despite evident ongoing proliferation at both d1 and d10.[12] Such differences in cellular response to ENU damage might also contribute to the increased tumor induction in the d1-treated group.

Focal lesions of persistent EGL in the subpial position were common in ptch1 mice and occasionally found in WT mice. In addition, the lesions of persistent EGL cells distributed diffusely or zonally in the molecular layer were induced by ENU in both mice. But, the incidence of persistent EGL cells did not correlate with medulloblastoma induction. Persistent EGL has been observed in other mutant mice, and it is believed that persistence of the EGL alone is not sufficient for tumorigenesis because none of the mutant mice showing persistent EGL other than ptch1 mice develop medulloblastoma.[20] Furthermore, morphological alterations like ectopic EGL cells were induced by chemicals such as methyl-azoxy-methanol and cisplatin during cerebellar histogenesis in rats and mice, along with disappearance of the basket cells or damage of glial fibers.[21,22] Because persistence of the EGL was found in both ptch1 and WT mice, this phenomenon may occur independently of the Shh-Ptch pathway, although damage of glia and basket cells was not apparent in our study. Misalignment of Purkinje cells was reported in rat cerebellum following prenatal exposure to X-irradiation, and the decrease in Reelin, which is expressed in the granule cell at a high level and helps regulating processes of neuronal migration and positioning in the developing brain, was thought to be a possible cause.[23] Therefore, misalignment of Purkinje cells observed in our study also may result from a marked decrease in EGL cells damaged by ENU.

Currently, human medulloblastomas are classified as four distinct subtypes by genomic approaches,[5,6] and future development of therapeutics and new drugs for medulloblastoma should take account of these subtypes. Tumors of ptch1 mice are thought to be equivalent for those of the SHH group in human, therefore, our model will be a useful tool for testing new drugs targeting the Shh pathway. Additionally, cerebellar development occurring after birth in mice is of good benefit for investigation of the effects of chemical exposure during development on medulloblastoma. Because medulloblastoma of ptch1 mice resembles human cases in histology, marker expression and cell origin, our model will be informative for human risk assessment of environmental chemicals and new drugs during development. In contrast, it should be recognized that ptch1 mouse is unsuitable for the research of medulloblastoma other than the SHH group. Also, this model might not be applicable for elucidation of onset of human medulloblastoma in some cases, because our model is developed for rapid screening of environmental chemicals and new drugs and there might be some differences between induced and spontaneous tumors at the molecular level.

In summary, ENU is available for the induction of medulloblastoma in ptch1 mice, and 10 mg of ENU administered on d1 was an appropriate dosing condition. Induction of medulloblastoma by ENU may be a good model for studying modifier effects on medulloblastoma tumorigenesis because this method allows for high tumor frequency and shorter latency and there was no occurrence of neural tumors other than medulloblastoma in the brain. This model will be helpful for human risk assessment of environmental chemicals and new drugs targeting the Shh pathway.

Acknowledgment

We thank Ms Tomomi Morikawa, Ayako Kaneko and Yoshimi Kosaka for technical assistance in conducting the animal study. This study was supported by Health and Labour Sciences Research Grants, Research on Risk of Chemical Substances, Ministry of Health, Labour and Welfare, Japan (H22-Toxicol-003).

Disclosure Statement

The authors have no conflict of interest.

doi: 10.1111/cas.12006

References

1 Packer RJ, Cogen P, Vezina G, Rorke LB. Medulloblastoma: clinical and biologic aspects. *Neuro Oncol* 1999; **1**: 232–50.
2 Bunin GR, Buckley JD, Boesel CP, Rorke LB, Meadows AT. Risk factors for astrocytic glioma and primitive neuroectodermal tumor of the brain in young children: a report from the Children's Cancer Group. *Cancer Epidemiol Biomarkers Prev* 1994; **3**: 197–204.
3 Shim YK, Mitsuhashi SP, van Wijngaarden E. Parental exposure to pesticides and childhood brain cancer: U.S. Atlantic coast childhood brain cancer study. *Environ Health Perspect* 2009; **117**: 1002–6.
4 Weng HH, Tsai SS, Wu TN, Sung FC, Yang CY. Nitrate in drinking water and the risk of death from childhood brain tumors in Taiwan. *J Toxicol Environ Health A* 2011; **74**: 769–78.
5 Northcott PA, Korshunov A, Witt H *et al*. Medulloblastoma comprises four distinct molecular variants. *J Clin Oncol* 2011; **29**: 1408–14.
6 Kool M, Korshunov A, Remke M *et al*. Molecular subgroups of medulloblastoma: an international meta-analysis of transcriptome, genetic aberrations, and clinical data of WNT, SHH, Group 3, and Group 4 medulloblastomas. *Acta Neuropathol* 2012; **123**: 473–84.
7 Behesti H, Marino S. Cerebellar granule cells: insights into proliferation, differentiation, and role in medulloblastoma pathogenesis. *Int J Biochem Cell Biol* 2009; **41**: 633–45.
8 Goodrich LV, Milenković L, Higgins KM, Scott MP. Altered neural cell fates and medulloblastoma in mouse patched mutants. *Science* 1997; **277**: 1109–13.
9 Wetmore C, Eberhart DE, Curran T. The normal patched allele is expressed in medulloblastoma from mice with heterozygous germ-line mutation of patched. *Cancer Res* 2000; **60**: 2239–46.
10 Corcoran RB, Scott MP. A mouse model for medulloblastoma and basal cell nevus syndrome. *J Neurooncol* 2006; **78**: 307–18.
11 Pazzaglia S, Mancuso M, Atkinson MJ *et al*. High incidence of medulloblastoma following X-ray-irradiation of newborn Ptch1 heterozygous mice. *Oncogene* 2002; **21**: 7580–4.
12 Pazzaglia S, Tanori M, Mancuso M *et al*. Linking DNA damage to medulloblastoma tumorigenesis in patched heterozygous knockout mice. *Oncogene* 2006a; **25**: 1165–73.
13 DiGiovanni J. Modification of multistage skin carcinogenesis in mice. *Prog Exp Tumor Res* 1991; **33**: 192–229.
14 Imaida K, Fukushima S. Initiation-promotion model for assessment of carcinogenicity: medium-term liver bioassay in rats for rapid detection of carcinogenic agents. *J Toxicol Sci* 1996; **21**: 483–7.
15 Vesselinovitch SD, Rao KV, Mihailovich N, Rice JM, Lombard LS. Development of broad spectrum of tumors by ethylnitrosurea in mice and the modifying role of age, sex, and strain. *Cancer Res* 1974; **34**: 2930–8.
16 Searle CE, Jones EL. The multipotential carcinogenic action of *N*-ethyl-*N*-nitrosourea administered neonatally to mice. *Br J Cancer* 1976; **33**: 612–25.
17 Pazzaglia S, Tanori M, Mancuso M *et al*. Two-hit model for progression of medulloblastoma preneoplasia in Patched heterozygous mice. *Oncogene* 2006b; **25**: 5575–80.
18 Thomas WD, Chen J, Gao YR *et al*. Patched1 deletion increases *N*-Myc protein stability via a mechanism of medulloblastoma initiation and progression. *Oncogene* 2009; **28**: 1605–15.
19 Wetmore C, Eberhart DE, Curran T. Loss of p53 but not ARF accelerates medulloblastoma in mice heterozygous for patched. *Cancer Res* 2001; **61**: 513–6.
20 Oliver TG, Read TA, Kessler JD *et al*. Loss of patched and disruption of granule cell development in a pre-neoplastic stage of medulloblastoma. *Development* 2005; **132**: 2425–39.
21 Yamanaka H, Obata K. Displaced granule cells in the molecular layer of the cerebellar cortex in mice treated with methylazoxymethanol. *Neurosci Lett* 2004; **358**: 131–6.
22 Pisu MB, Roda E, Guioli S, Avella D, Bottone MG, Bernocchi G. Proliferation and migration of granule cells in the developing rat cerebellum: cisplatin effects. *Anat Rec A Discov Mol Cell Evol Biol* 2005; **287**: 1226–35.
23 Bermann W, Inouye M, Takagishi Y, Ogawa M, Mikoshiba K, Murata Y. Derangement of Purkinje cells in the rat cerebellum following prenatal exposure to X-irradiation: decreased Reelin level is a possible cause. *J Neuropathol Exp Neurol* 2010; **69**: 251–62.

J Toxicol Pathol 2012; 25: 241–247

Original Article

Involvements of Estrogen Receptor, Proliferating Cell Nuclear Antigen and p53 in Endometrial Adenocarcinoma Development in Donryu Rats

Midori Yoshida[1]*, Shin-ichi Katsuda[2], and Akihiko Maekawa[3]

[1] Division of Pathology, National Institute of Health Sciences, 1-18-1 Kamiyoga, Setagaya-ku, Tokyo 158-8501, Japan
[2] Department of Biological Safety Research, Japan Food Research Laboratories, 3-3 Bunkyo, Chitose-shi, Hokkaido 066-0052, Japan
[3] Chemical Management Center, National Institute of Technology and Evaluation, 2-24-9 Nishihara, Shibuya-ku, Tokyo 151-0066, Japan

Abstract: Involvements of estrogen receptor (ER)α, proliferating cell nuclear antigen (PCNA) and p53 in the uterine carcinogenesis process in Donryu rats, a high yield strain of the uterine cancer were investigated immunohistochemically. ERα was expressed in atypical endometrial hyperplasia, accepted as a precancerous lesion of the uterine tumors, as well as well- and in moderately-differentiated endometrial adenocarcinomas, and the intensities of expression were similar to those in the luminal epithelial cells of the atrophic uterus at 15 months of age. The expression, however, was negative in the tumor cells of poorly differentiated type. Good growth of implanted grafts of the poorly-differentiated adenocarcinomas in both sexes with or without gonadectomy supported the estrogen independency of tumor progression to malignancy. PCNA labeling indices were increased with tumor development from atypical hyperplasia to adenocarcinoma. The tumor cells in poorly-differentiated adenocarcinomas were positive for p53 positive but negative for p21 expression, suggesting accumulation of mutated p53. These results indicate that the consistent ERα expression is involved in initiation and promotion steps of uterine carcinogenesis, but not progression. In addition, PCNA is related to tumor development and the expression of mutated p53 might be a late event during endometrial carcinogenesis. (DOI: 10.1293/tox.25.241; J Toxicol Pathol 2012; 25: 241–247)

Key words: Endometrial adenocarcinoma Donryu, rat, ERα, PCNA, p53

Introduction

Naturally occurring endometrial adenocarcinomas are rare in rats, whereas inductions of uterine adenocarcinomas have been reported in some safety evaluation studies[1–3]. The mechanisms of rat uterine cancer development are not fully determined; however, estrogens are accepted to play a crucial role in the development in rodents[4–6] as well as endometrioid adenocarcinomas in humans[11,12]. Maekawa and co-workers[13] found a high-occurrence of spontaneous uterine endometrial adenocarcinomas in aged Donryu rats, which are similar to human cases as follows: 1) multistep development of uterine lesions from atypical hyperplasias to adenocarcinomas; 2) ovarian hormonal imbalance especially elevation of the serum 17β-estradiol (E2) level relative to progesterone, which manifests as atrophic ovaries with cystic follicles and lack of a corpus luteum and 3) morphologic similarities to endometrioid adenocarcinomas of humans[11, 12]. The high yield of endometrial adenocarcinomas in Donryu rats is considered to be closely linked to earlier occurrence of the ovarian imbalance detected as persistent estrus by vaginal smear[14].

Based on these characteristics, a 2-stage uterine carcinogenesis model was established with intrauterine treatment of *N*-ethyl-*N'*-nitro-*N*-nitrosoguanidine (ENNG) using this rat strain[15] to detect promoting or preventive effects of test chemicals[16–18].

In humans, endometrial adenocarcinoma is the most common malignant tumor of the female genitals in developed countries. The tumors are fundamentally sub-classified into two types, type I, endometrioid adenocarcinoma and type II, serous carcinoma based on epidemiological, clinico-pathological and molecular findings[11,12,19,21]. The former, the most common type, is considered to be related excess estrogen exposure, developing from endometrial glandular hyperplasia (AH). In contrast, the latter, accounting for a minority of endometrial carcinomas, does not seem to be related to estrogenic risk factors or elevated serum hormone levels. The estrogen receptor (ER) can usually be

Received: 25 April 2012, Accepted: 3 July 2012
*Corresponding author: M Yoshida (e-mail: midoriy@nihs.go.jp)

identified in endometrioid adenocarcinomas, whereas serous lesions are generally negative[11,22]. In addition, mutations in the p53 tumor suppressor gene and accumulation of p53 protein have been detected in approximately 90% of serous carcinomas[12,23,24], whereas they are not common in endometrioid adenocarcinomas and AH[12,25]. In the endometrial adenocarcinomas in Donryu rats, however, the role of ERα and other molecular pathology in uterine carcinogenesis has hitherto been obscure in this model except for K-*ras* point mutaions[26].

The present study was conducted to determine the expression profile of ERα as well as the mutation of p53 during development of endometrial adenocarcinomas in Donryu rats and its link to immunohistochemically determined cellular proliferative activity and p53 protein expression. Furthermore, to confirm hormone-independency in poorly differentiated endometrial adenocarcinomas in Donryu rats, some tumor grafts were implanted into the back subcutis of female and male rats, with or without gonadectomy, and growth of the grafts was assessed.

Materials and Methods

Samples obtained

The numbers of normal tissue samples and proliferative lesions in the endometrium of the uteri examined are shown in Table 1. Uterine samples were obtained from aged Donryu rats with or without various proliferative lesions (97 rats, 12 to 15 months of age) used in uterine carcinogenicity studies previously. The aged normal uterus and proliferative lesions including well- or poorly differentiated adenocarcinomas were treated with intrauterine administrations of ENNG (Nakalai Tesque, Kyoto, Japan) at 10 or 11 weeks of age using assays of uterine carcinogenicity. The tissues were fixed in 10% neutral buffered formaldehyde solution and embedded in paraffin. The specimens were routinely processed and stained with hematoxylin-eosin (HE) for histopathological classification.

After fixation, the upper, middle and lower parts of each uterine horn and the cervix of all uteri were dissected into 3 pieces in cross section to classify uterine proliferative lesions into three degrees of atypical hyperplasia (slight, moderate or severe) and adenocarcinomas, according to the criteria described previously[4,14]. Briefly, atypical hyperplasia is defined as irregular proliferation of atypical glands in the endometrium, and adenocarcinomas were diagnosed on the basis of invasion of the atypical glands into the muscularis. The adenocarcinomas were divided into well-, moderately- and poorly-differentiated by morphological malignancy and degree of invasion: limited to the uterus, invading into the serosa and/or surrounding adnexae, and with distant metastasis, in accordance with the simplified FIGO histopathological grades for human uterine cancers[27]. Specimens from other reproductive tracts or representative organs were examined microscopically.

Immunohistochemistry

Serial sections of the uterus and various neoplastic lesions were incubated with the following antibodies: ERα (catalog No. NCL-ER-LH2; dilution at ×50; NovoCastra Laboratories Ltd, Newcastle, UK), proliferating cell nuclear antigen (PCNA, catalog No. M0879; dilution at ×150; DakoCytomation, Kyoto, Japan), anti-wild and mutant p53 (catalog No. NCL-p53-CM5p; dilution at ×200; NovoCastra Laboratories Ltd, Newcastle, UK) or p21 (catalog No. sc6246; dilution at ×100; Santa Cruz Biotechnology, Inc, California, USA). Before the incubation, the sections were heated with citrate buffer pH 7.0 using a microwave (antibodies against ERα, PCNA, p53 or p21 for 20, 2, 20 or 20 min, respectively). After the incubation with these antibodies during overnight at 4°C, the sections were processed using peroxidase labeled dextran polymers (Histofine, Nichirei, Tokyo, Japan) and were visualized with 3,3'-diaminobenzidine tetra hydrochloride (Wako Pure Chemical Industries, Osaka, Japan). Counterstaining was with hematoxylin. The uterus at proestrus in the normal cycling rat was used as a positive control for the ERα, PCNA and p21 antibodies. Repeated positive reactions in the nuclei of different poorly-differentiated endometrial adenocarcinoma cells were judged as positive. Sections incubated without these antibodies were used as the negative control.

Image-analysis of expression profiles

To compare ERα, PCNA and p53 immunohistochemical expression profiles in the endometrium of normal uteri in aged female rats with those of atypical hyperplasia and adenocarcinomas, the positive areas for these antibodies in total nuclear areas in the epithelium and lesions were calculated using an image analyzing system (IPAP, Sumika Technos, Osaka, Japan). After confirmation of the morphological features of each lesion by HE staining, the positive nuclear areas for these antibodies and total nuclear areas in

Table 1. Numbers of Uterine Samples Examined in the Present Study

Samples obtained	Number of samples
Normal areas	
Normal uteri showing no cyclicity (at 12 to 15 months of age)	50
Proliferative lesions	
Atypical hyperplasias (slight to severe, at 12 to 15 months of age) 27, 26 and 24 samples for slight, moderate and severe, respectively)	67
Adenocarcinomas (at 12 to 15 months of age, 28 well-differentiated and 3 moderately-differentiated)	31
Adenocarcinomas (poorly differentiated, at 12 to 15 months of age)	8

4 specimens of normal uteri and each lesion were counted, and the percentages of positive areas for the antibodies were calculated. The typical changes in the normal uteri and each lesion were determined using an automated cellular image analysis scanning system (SL-50, Applied imaging, Santa Clara, CA, USA). In addition, immunohistochemical staining with p21 antibody was performed if tumor cells were stained positive for p53.

Confirmation of hormone independence of poorly-differentiated endometrial adenocarcinomas by tumor graft implantation

Mature male and female Crj:Donryu rats demonstrating normal cycling were purchased from Charles River Laboratories Japan (Kanagawa, Japan) and maintained in an air-conditioned animal room. Commercial pellet diet (CRF-1, Oriental Yeast, Kanagawa, Japan) and drinking water were available *ad libitum* throughout the experiment. Half of the male and female rats (6 to 9 animals per sex) were gonadectomized under deep anesthesia. Two or 3 weeks after the gonadectomy, small grafts (3 mm cubes) from one poorly differentiated endometrial adenocarcinoma were implanted into the back subcutis of normal (gonad-intact) and gonadectomized animals. Two carcinomas identified as immunohistochemistry as ERα negative were selected from 4 samples. Growth of the grafts was checked daily by palpation and measured once a week up to 6 weeks after the implantation. Animal care and use followed the guide of the Animal Committee of Sasaki Institute.

Statistical analysis

Means and standard deviations (SD) of the individual values of positive nuclear areas and total nuclear areas in the normal uteri and each lesion were calculated. Growth of the grafts in the intact females was compared with those in other groups. In multiple comparisons, continuous data were analyzed with Barlett's test. When variances were homogenous, Dunnett's multiple comparison test was performed. The Steel's multiple comparison test was employed, when variances were not homogenous. The level of significance was set as $P<5\%$ and 1%.

Results

Histopathologic changes in atypical hyperplasias and adenocarcinomas dependent were similar among the samples obtained, respectveily. Well-differentiated adenocarcinomas were characterized by the tumor cells arranged glandular or back-to-back pattern and cytoplasmic vacuolation was partly detected in some cases. In poorly differentiated ones, severe cellular atypia and structure destruction with cirrhosis including dissemination into the abdominal cavity or metastasis to the lungs were frequently observed.

Typical immunohistochemical profiles for ERα, PCNA and p53 in uterine proliferative lesions assessed using an automated cellular image analyzing system are shown in Fig. 1, and calculated percentage values for positive cells are shown in Fig. 2. ERα expression was constantly observed in most of the uterine epithelium in aged rats. In the aged uteri, severe fibrosis or cystic hyperplasia was common, so the glandular epithelium was often difficult to detect. ERα positive tumor cells were distributed in the atypical hyperplasias and well- and moderately-differentiated adenocarcinomas. Their intensities were similar to that in the aged uterus (Fig. 2). In clear contrast, no binding was detected in any of the poorly differentiated adenocarcinomas examined.

The numbers of PCNA-positive cells were elevated in uterine proliferative lesions, compared with the normal epithelia, and there was a tendency for an increase in the degree of atypical hyperplasia, and significantly increase in the adenocarcinomas with advancing malignancy (Fig. 1 and Fig. 2). There was no expression of p53 in normal epithelia and well- or moderately-differentiated adenocarcinomas of either the early and advanced types. On the other hand, strong antibody binding was evident in poorly differentiated adenocarcinomas, especially in cells with marked cellular atypia in invading areas, with or without abundant fibrous stroma, although p21 expression was not detectable in any tumor cells from poorly differentiated adenocarcinomas that were positive for p53.

Growth curves for implanted tumors are shown in Fig. 3. The tumor nodules grafted into the back skin showed rapid growth in all animals of both sexes, becoming detectable as palpable nodules after 2 weeks. The growth curves did not differ between males and females up to 6 weeks after the implantation and were not influenced by gonadectomy. In addition, metastasis to the lung and/or lymph nodes was observed in any groups with similar incidences (over 80%) at the termination.

The most common aging-associated changes in the endometrium were stromal fibrosis, cystic hyperplasia of the luminal epithelium, squamous metaplasia, atrophic cuboidal epithelium and inflammation. The ovaries of aged rats in the present study showed atrophic changes with lack of corpus lutea, cystic or atretic follicles and increased interstitial glands, which are typical of the observations for aged ovaries in this strain. A number of age-related nonneoplastic or neoplastic lesions were observed in other organs, but no clear relationship with the expression profiles of ERα, PNCA or p53 could be established.

Discussion

E2 plays a crucial role in proliferating activity in the uteri via ER in mammals[28–31]. In our previous studies, chronic exposure to estrogenic compounds or long-term elevation of the serum E2/progesterone ratio has enhanced the development of uterine neoplastic lesions in rats, whereas the lesions were not inducible in ovariectomized rats[7–9,32].

The present results of consistent ERα expression in the majority of the normal endometrial epithelium in aged uteri, uterine atypical hyperplasias and well- to moderately differentiated adenocarcinomas suggest that uterine proliferating lesions in rats were estrogen dependent event mediated by

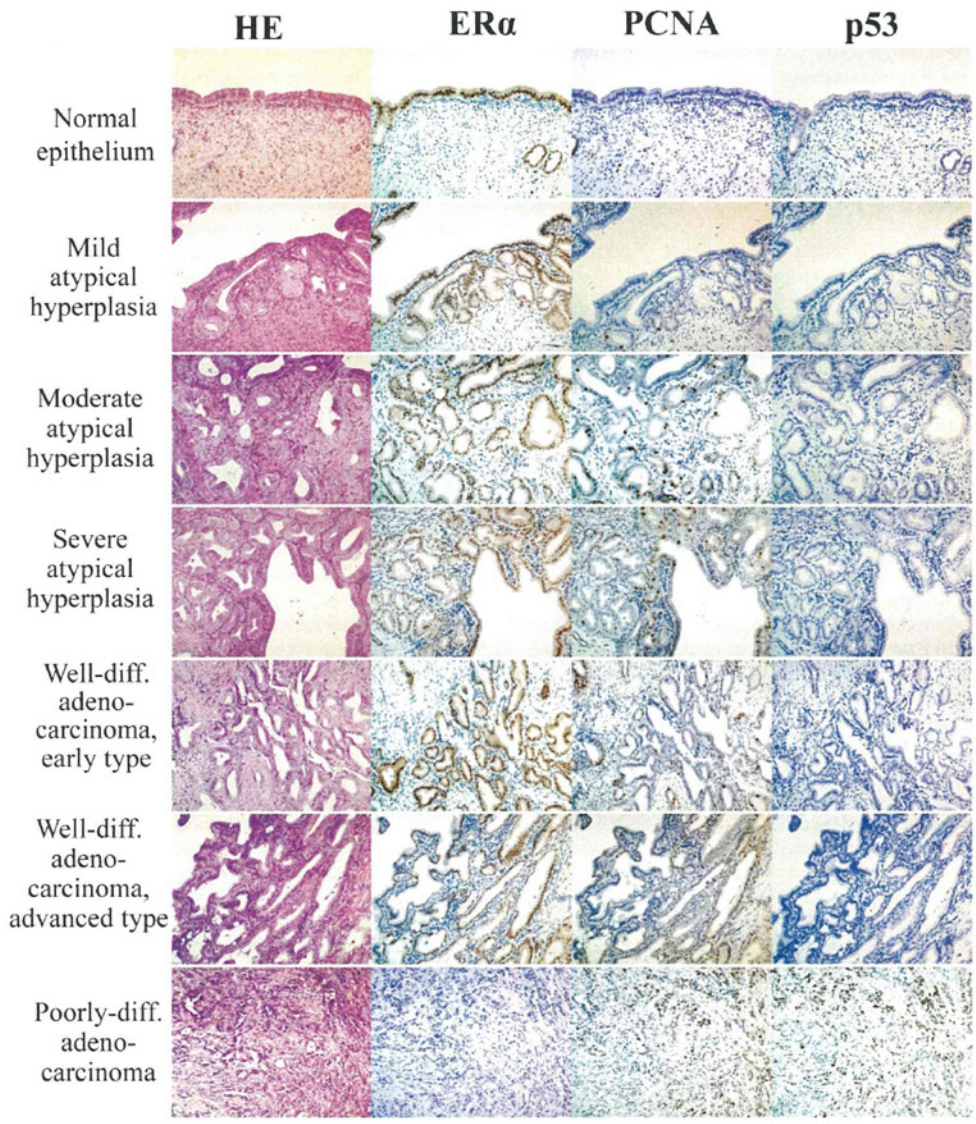

Fig. 1. Immunohistochemical expression profiles of ERα, PCNA and p53 and HE staining in representative areas of normal uteri (at 12 to 15 months of age) and various neoplastic lesions in the uteri. Well-diff., well-differentiated adenocarcinoma; Poorly-diff., poorly-differentiated adenocarcinomas.

ERα. The high yield of endometrial adenocarcinomas in the Donryu rats is considered to be linked to continuous stimulation of E2, and our results added that ERα-expressing cells might be necessary for the initiation and promotion steps of uterine adenocarcinoma development. The loss of ERα in poorly differentiated adenocarcinomas supported by estrogen-independent growth of the implanted tumors might indicate that the expression of ERα is not necessary for the progression step of uterine cancer in rats. It has already been established for human endometrial adenocarcinomas that hormone therapy has no effect on advanced malignancies[33, 34]. The involvement of another estrogen re-

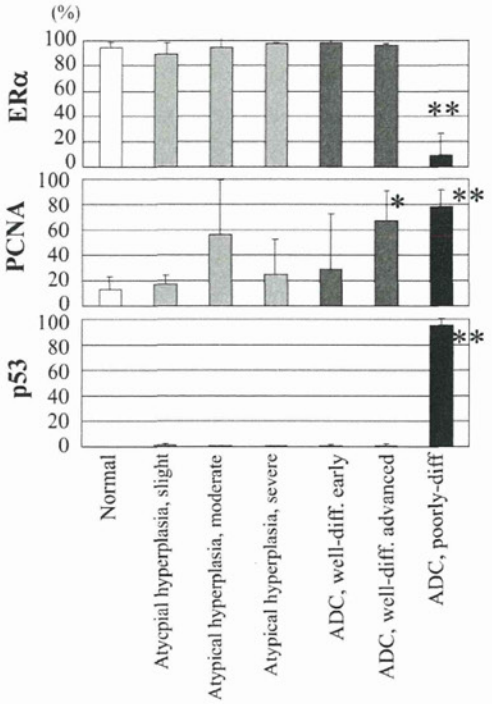

Fig. 2. Percentages of immunohistochemically positive cells for ERα, PCNA and p53 in representative areas of normal uteri (at 15 months of age) and various neoplastic lesions in the uteri. *P<0.05 and **P<0.01 indicate significant differences in the expression of endometrial epithelium (normal) and uterine proliferative lesions compared with that in normal aged rats at 5% and 1%, respectively. The column and bar are represent the mean and SD, respectively.

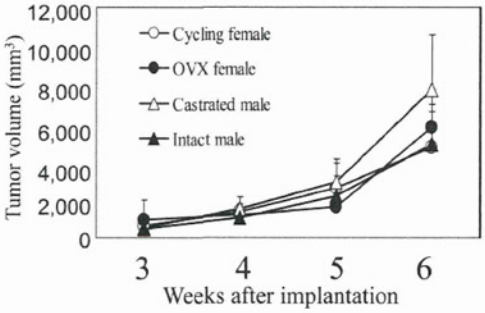

Fig. 3. Growth curves of tumor grafts after implantation. OVX, ovariectomy.

ceptor form, ERβ, to uterine cancer development in rodents remains to be established, but recent investigations have pointed to a relationship between ERα and β expression in human endometrial adenocarcinomas[35,36].

In the present study, the PCNA labeling index was increased in advanced proliferating lesions, correlating with cellular atypia and/or tumor invasion. Only the poorly-differentiated tumors were positive for p53 accumulation, and their negative reactions for p21 suggested that the cells positive for p53 were mutated. In endometrial adenocarcinomas in women, mutation in the p53 tumor suppressor gene and accumulation of p53 protein are detected in approximately 90% of serous adenocarcinomas[11,12]. In endometrioid adenocarcinomas, p53 expression is not common, but the p53 accumulation is considered to indicate progression to uterine carcinoma or large high-grade tumors[11,19]. It was recently reported that p53 is not related to ERα expression status in women[37], but any links to the question in rodents remain to be clarified.

Endometrial adenocarcinomas in humans have been classified into two broad categories: type I estrogen-dependent adenocarcinoma with an endometriod morphology and type II non-estrogen-dependent adenocarcinoma with a serous, papillary or clear cell morphology[11,12,19–21]. The present study and our previous studies described in the introduction indicate that the endometrial adenocarcinomas in the Donryu rat strain have many similarities to type I, endometrioid adenocarcinoma in women. Samuelson *et al.* reported that spontaneous endometrial adenocarcinomas in BDII rats are also similar to type I tumors in women[38]. On the other hand, a possibility might exist that the poorly differentiated types in the present study might be biologically different from well-differentiated adenocarcinomas, because of the similarity of the p53 profile in the poorly-differentiated adenocarcinomas in rats to that of type II carcinomas in women. Whereas type I cancer develops in menopausal women, type II is mainly detected in elderly women[11]. Further investigation might be required to clarify the suggestion above; however, the samples of adenocarcinomas in the present study were obtained from rats at similar ages supporting the idea that poorly-differentiated adenocarcinoma represent the late stage of well- or moderate-differentiated adenocarcinomas.

In conclusion, the present study provided evidence of the involvement of consistent ERα expression in the initiation and promotion steps of uterine carcinogenesis in rats. The loss of expression was linked to malignant progression and hormone independence. PCNA is related to tumor development and the expression of p53 might be a late event leading to malignancy. The data point to a number of similarities with endometrioid adenocarcinomas, the major type of corpus uterine cancer in women.

Acknowledgments: We sincerely thank Mr. Yutaka Hatanaka and Mr. Takuji Mihara (BioMedical Science Department, DakoCytomation Co., Ltd. Kyoto, Japan) for their special technical supports the image analysis system for immunohistochemical sections, and Ms. Asako H and Ms. Kajiwara C for preparation of samples for histopathological examination. The present study was partly supported

by Health and Labor Science Research Grants for Risk of Chemical Substances from Ministry of Health, Labor and Welfare (H22-Toxicol-003).

References

1. Pintér A, Torok G, Borzsonyi M, Surjan A, Csik M, Kelecsenyi Z, and Kocsis Z. Lon-term carcinogenicity bioassay of the herbicide atrazine in F344 rats. Neoplasma. **37**: 533–544. 1990. [Medline]
2. Irwin RD, Haseman JK, and Eutis SL. 1,2,3-Trichloropropane: a multiple carcinogen in rats and mice. Fundam Appl Toxicol. **25**: 241–252. 1995. [Medline] [CrossRef]
3. Picut CA, Aoyama H, Holder JW, Gold LS, Maronpot RR, and Dixon D. Boromoethane, chloroethane and ethylene oxide induced uterine neoplasms in B6C3F1 mice from 2-year NTP inhalation bioassays: pathology and incidence data revised. Exp Toxicol Pathol. **55**: 1–9. 2003. [Medline] [CrossRef]
4. Nagaoka T, Takeuchi M, Onodera H, Matsushima Y, Ando-Lu J, and Maekawa A. A sequential observation of spontaneous endometrial adenocarcinoma development in Donryu rats. Toxicol Pathol. **22**: 261–269. 1994. [Medline] [CrossRef]
5. Niwa K, Murase T, Mirishita S, Tanaka T, Mori H, and Tamaya T. Enhancing effect of estrogens on endometrial carcinogenesis initiated by N-methyl-N-nitrosourea in ICR mice. Jpn J Cancer Res. **84**: 951–955. 1993. [Medline] [CrossRef]
6. Niwa K, Tanaka T, Yokoyama Y, Mori H, and Tamaya T. Rapid induction of endometrial carcinoma in ICR mice treated with N-methyl-N-nitrosourea and 17B-estradiol. Jpn J Cancer Res. **82**: 1391–1396. 1991. [Medline] [CrossRef]
7. Nagaoka T, Takeuchi M, Onodera H, Mitsumori K, Lu J, and Maekawa A. Experimental induction of uterine adenocarcinoma in rats by estrogen and N-methyl-N-nitrosourea. In vivo. **7**: 525–530. 1993. [Medline]
8. Maekawa A, Takahashi M, Ando J, and Yoshida M. Uterine carcinogenesis by chemicals/hormones in rodents. J Toxicol Pathol. **12**: 1–11. 1999. [CrossRef]
9. Katsuda S, Yoshida M, Kuroda H, Ando J, Takahashi M, Kurokawa Y, Watanabe G, Taya K, and Maekawa A. Uterine adenocarcinoma in N-ethyl-N'-nitro-N-nitrosoguanidine-treated rats with high-dose exposure to p-terty-octylphenol during adulthood. Jpn J Cancer Res. **93**: 117–124. 2002. [Medline] [CrossRef]
10. Maekawa A, Yoshida M, Katsuda S-I, and Imai K. Toxicologic/carcinogenic effects of endocrine disrupting chemicals on the female genital organs of rodents. J Toxicol Pathol. **17**: 69–83. 2004. [CrossRef]
11. Sherman ME. Theories of endometrial carcinogenesis: a multidisciplinary approach. Mod Pathol. **13**: 295–308. 2000. [Medline] [CrossRef]
12. Albertini AF, Devouassoux-Shesheboran M, and Genesite C. Pathology of endometrioid carcinoma. Bull Cancer. **99**: 7–12. 2012. [Medline]
13. Maekawa A, Onodera H, Tanigawa H, Furuta K, Kanno J, Matsuoka C, Ogiu T, and Hahashi Y. Spontaneous neoplastic and non-neoplastic lesions in aging Donryu rats. Jpn J Cancer Res. **77**: 882–890. 1986. [Medline]
14. Nagaoka T, Onodera H, Matsushima Y, Todate A, Shibutani M, Ogasawara H, and Meakawa A. Spontaneous uterine adenocarcinomas in aged rats and their relation to endocrine imbalance. J Cancer Res Clin Oncol. **116**: 623–628. 1990. [Medline] [CrossRef]
15. Ando-Lu J, Takahashi M, Imai S, Ishihara R, Kitamura T, Iijima T, Takano S, Nishiyama K, Suzuki K, and Maekawa A. High-yield induction of endometrial adenocarcinomas in Donryu rats by a single intra-uterine administration of N-ethyl-N'-nitro-N-nitrosoguanidine. Jpn J Cancer Res. **85**: 789–793. 1994. [Medline] [CrossRef]
16. Nishiyama K, Ando-Lu J, Nishimura S, Takahashi M, Yoshida M, Sasahara K, Miyajima K, and Maekawa A. Initiating and promoting effects of concurrent oral administration of ethylenethiourea and sodium nitrite on uterine endometrial adenocarcinoma development in Donryu rats. In vivo. **12**: 363–368. 1998. [Medline]
17. Yoshida M, Kudoh K, Katsuda S, Takahashi M, Ando J, and Maekawa A. Inhibitory effects of uterine endometrial carcinogenesis in Donryu rats by tamoxifen. Cancer Lett. **134**: 43–51. 1998. [Medline] [CrossRef]
18. Katsuda S, Yoshida M, Saarinen N, Smeds A, Nakae D, Santti R, and Maekawa A. Chemopreventive effects of hydorxymatairesinol on uterine carcinogenesis in Donryu rats. Exp Bio Med. **229**: 417–424. 2004.
19. Abal M, Planaguma J, Gill-Moreno A, Monge M, Ganzales M, Baro T, Garcia A, Castellvi J, Cajal SR, Xercavinzs J, Alameda F, and Reventos J. Molecular pathology of endometrial carcinoma: transcriptional signature in endometrioid tumors. Histol Histopathol. **21**: 197–204. 2006. [Medline]
20. Cerezo L, Cárdenes H, and Michael H. Molecular alterations in the pathogenesis of endometrial adenocarcinoma. Therapeutic implications. Clin Transl Oncol. **8**: 231–241. 2006. [Medline] [CrossRef]
21. Doll A, Abai M, Rigau M, Monge M, Gonzales M, Demajo S, and Colás E, Llauradó M, Alazzouzi H, Ianagumá J, Lohmann MA, Garcia J, Roman CJ, Gil-Moreno A, Xercavins J, Alameda F, and Reventós J. Novel molecular profiles of endometrial cancer-new light through old windows. J Steroid Mol Biol. **108**: 221–229. 2008. [CrossRef]
22. Halperin R, Zehavi S, Habler L, Hades E, Bukovsky I, and Schneider D. Comparative immunohistochemical study of endometrioid and serous papillary carcinoma of endometrium. Eur J Gynaecol Oncol. **22**: 122–126. 2001. [Medline]
23. Tashiro H, Isacson C, Levine R, Kurman RJ, Cho KR, and Kedrick L. p53 Gene mutations are common in uterine serous carcinoma and occur early in their pathogenesis. Am J Pathol. **150**: 177–185. 1997. [Medline]
24. Demopoulos RI, Mesia AF, Mittal K, and Vamvakas E. Immunohistochemical comparison of uterine papillary serous and papillary endometrioid carcinoma: clues to pathogenesis. Int J Gynecol Pathol. **18**: 233–237. 1999. [Medline] [CrossRef]
25. Sherman ME, Bur ME, and Kurman RJ. p53 in endometrial cancer and its putative precursors: evidence for diverse pathways of tumorigenesis. Hum Pathol. **26**: 1268–1274. 1995. [Medline] [CrossRef]
26. Tanoguchi K, Yaegashi N, Jiko K, Maekawa A, Sato S, and Yajima A. K-ras point mutations in spontaneously occurring endometrial adenocarcinomas in the Donryu rat. Tohoku J Exp Med. **189**: 87–93. 1999. [Medline] [CrossRef]

27. Pecorelli S, Benedet JL, Creasman WT, and Shepherd JH. FIGO staging of gynecologic cancer. Int J Gynaecol Obstet. **64**: 5–10. 1999. [Medline] [CrossRef]
28. Ando-Lu J, Sasahara K, Nishiyama K, Takano S, Takahashi M, Yoshida M, and Maekawa A. Stain-differences in proliferative activity of uterine endometrial cells in Donryu and Fischer 344 rats. Exp Toxicol Pathol. **50**: 185–190. 1998. [Medline] [CrossRef]
29. Katsuda SI, Yoshida M, Watanabe T, Kuroda H, Ando-Lu J, Takahashi M, Hayashi H, and Maekawa A. Estrogen receptor mRNA in uteri of normal estrous cycling and ovariectomized rats by in situ hybridization. Proc Soc Exp Biol Med. **221**: 207–214. 1999. [Medline] [CrossRef]
30. Yoshida M, Katsuda S, Ando J, Kuroda H, Takahashi M, and Maekawa A. Subcutaenous treatment of p-tert-octylphenol exerts estrogenic activity on the female reproductive tract in normal cycling rats of two different strains. Toxicol Lett. **116**: 89–101. 2000. [Medline] [CrossRef]
31. Cooke PS, Buchanan DL, Young P, Setiawan T, Brody J, Korach KS, and Taylor J. Stromal estrogen receptors mediate mitogenic effects of estradiol on uterine epithelium. Proc Natl Acad USA. **94**: 6535–6540. 1997. [CrossRef]
32. Yoshida M, Katashima S, Ando J, Tanaka T, Uematsu F, Nakae D, and Maekawa A. Dietary indole-3-carbinol promotes endometrial adenocarcinoma development in rats initiated with N-ethyl-N'-nitro-N-nistrosoguanidine, with induction of cytochrome P450s in the liver and consequent modulation of estrogen metabolism. Carcinogenesis. **25**: 2257–2264. 2004. [Medline] [CrossRef]
33. Pertschuk LP, Masood S, Simone J, Feldman JG, Fruchter RG, Axiotis CA, and Greene GL. Estrogen receptor immunohistochemistry in endometrial carcinoma: a prognostic marker for survival. Gynecol Oncol. **63**: 28–33. 1996. [Medline] [CrossRef]
34. Susumu N, Aoki D, Suzuki N, and Nozawa S. Hormonal therapy for endometrial adenocarcinoma. Gan To Kagaku Ryoho. **28**: 934–945 (Abstract in English) 2001. [Medline]
35. Utsunomiya H, Suzuki T, Harada N, Ito K, Matsuzaki S, Konno R, Sato S, Yajima A, and Sasano H. Analysis of estrogen receptor α and β in endometrial carcinomas: correlation with ERβ and clinicopathologic findings in 45 cases. Int J Gynecol Pathol. **19**: 335–341. 2000. [Medline] [CrossRef]
36. Takama F, Kanuma T, Wang D, Kagami I, and Mizunuma H. Oestrogen receptor β expression and depth of myometrial invasion in human endometrial cancer. Br J Cancer. **84**: 545–549. 2001. [Medline] [CrossRef]
37. Maeda K, Tsuda H, Hashiguchi Y, Yamamoto K, Inoue T, Ishiko O, and Ogita S. Relationship between p53 pathway and estrogen receptor status in endometrial-type endometrial cancer. Human Pathol. **33**: 386–391. 2002. [CrossRef]
38. Samuelson E, Hedberg C, Nilsson S, and Behboudi A. Molecular classification of spontaneous endometrial adenocarcinomas in BDII rats. Endocr Relat Cancer. **16**: 99–111. 2009. [Medline] [CrossRef]

Toxicologic Pathology, 00: 1-8, 2012

ISSN: 0192-6233 print / 1533-1601 online
DOI: 10.1177/0192623312464305

Differential Morphological Effects in Rat Corpora Lutea among Ethylene Glycol Monomethyl Ether, Atrazine, and Bromocriptine

Yoshikazu Taketa[1,2], Kaoru Inoue[1], Miwa Takahashi[1], Jyoji Yamate[2], and Midori Yoshida[1]

[1]*Division of Pathology, National Institute of Health Sciences, Tokyo, Japan*
[2]*Laboratory of Veterinary Pathology, Life and Environmental Sciences, Osaka, Japan*

Abstract

Ethylene glycol monomethyl ether (EGME) or atrazine induces luteal cell hypertrophy in rats. Our previous study suggested that EGME stimulates both new and old corpora lutea (CL), while atrazine stimulates new CL. Bromocriptine (BRC) is known to suppress the luteolysis in rats. This study investigated the light- and electron-microscopic luteal changes induced by EGME, atrazine, or BRC. Female rats were treated with EGME (300 mg/kg/day), BRC (2 mg/kg/day), EGME and BRC (EGME + BRC), or atrazine (300 mg/kg/day) for 7 days. Luteal cell hypertrophy induced by EGME, EGME + BRC, and atrazine was subclassified into the following two types: CL hypertrophy, vacuolated type (CL-V) characterized by intracytoplasmic fine vacuoles, and CL hypertrophy, eosinophilic type (CL-E) characterized by eosinophilic and abundant cytoplasm. The proportions of CL-V and CL-E were different among the treatments. BRC-treated old CL showed lower proportion of endothelial cells and fibroblasts than normal old CL. Ultrastructural observation revealed that the luteal cells of CL-V contained abundant lipid droplets, whereas those of CL-E in EGME and EGME + BRC groups showed uniformly well-developed smooth endoplasmic reticulum. No clear ultrastructural difference was observed between the control CL and atrazine-treated CL-E. These results indicate that EGME, atrazine, and BRC have differential luteal morphological effects.

Keywords: corpora lutea; ovarian toxicity; ethylene glycol monomethyl ether; atrazine; bromocriptine; rats.

Introduction

There is growing interest in the possible health threat posed by substances in the environment, food, and consumer products that interfere with reproductive function (Yuan and Foley 2002). The female reproductive organs are regulated across the estrous cycle by the hypothalamic–pituitary–gonadal (HPG) system through complex feedback loops. These feedback mechanisms are perturbed by ovarian toxicants including ethylene glycol monomethyl ether (EGME), atrazine, and bromocriptine (BRC) (Kumazawa et al. 2009; Taketa et al. 2011a). In rodents, ovarian toxicants produce abnormal hormone secretion, disrupted estrous cycles, and identifiable histopathological changes in the reproductive tract; and detailed histopathological evaluations often lead to their mode of actions (Sanbuissho et al. 2009).

EGME and atrazine induce luteal hypertrophy following repeated administration (Davis et al. 1997; Taketa et al. 2010, 2011a). EGME, which is widely used in various industrial products such as detergents, adversely affects both the male and female reproductive systems (Johanson 2000; Welsch 2005). In the female reproductive system, EGME and its active metabolite, 2-methoxy acetic acid (MAA), induce the hypersecretion of progesterone (P4) from luteal cells both *in vivo* and *in vitro* (Almekinder et al. 1997; Davis et al. 1997; Taketa et al. 2011a). Atrazine, a chlorotriazine herbicide, is a potent endocrine disruptor that promotes mammary tumor growth in female rats (Eldridge et al. 1994) and alters the central nervous system regulation of the reproductive system in mammals (Cooper et al. 2000; Eldridge et al. 1999; Foradori et al. 2009). Recently, atrazine has been shown to stimulate steroidogenesis and increase P4 secretion *in vitro* and *in vivo* (Fraites et al. 2009; Tinfo et al. 2011).

BRC, a dopamine D2 agonist that inhibits prolactin (PRL) release in the anterior pituitary, is also known to affect luteal function in rats (Gaytan et al. 2001). In rats, BRC suppresses luteolysis and induces an increase in the number of corpora lutea (CL) without affecting the estrous cycle (Gaytan et al. 2001; Kumazawa et al. 2009).

Rodents, including rats and mice, have features that do not form a truly functional CL during the ovarian cycle unless mating results in pseudopregnancy or pregnancy (Stouffer 2006). In rats, CL are classified into two main types: new CL, which are newly formed by the current ovulation, and old CL, which are CL remaining from prior estrous cycles (Bowen and Keyes 2000). These types of CL are generated and regress over several cycles. New and old CL are morphologically distinguishable at

The authors declared no potential conflicts of interest with respect to the research, authorship, and/or publication of this article.

The authors disclosed receipt of the following financial support for the research, authorship, and/or publication of this article: This work was partly supported by Health and Labour Sciences Research Grants for Risk Chemical Substances from the Ministry of Health, Labour and Welfare, Japan [H22-Toxicol-003].

Address correspondence to: Yoshikazu Taketa, Division of Pathology, National Institute of Health Sciences, 1-18-1 Kamiyoga, Setagaya-ku, Tokyo 158-8501, Japan; e-mail: y-taketa@nhc.eisai.co.jp.

Abbreviations: CL, corpora lutea; EGME, ethylene glycol monomethyl ether; MAA, 2-methoxy acetic acid; BRC, bromocriptine; P4, progesterone; PRL, prolactin; HPG, hypothalamic–pituitary–gonadal; H&E, hematoxylin and eosin; RT, room temperature; DW, distilled water; SER, smooth endoplasmic reticulum; RER, rough endoplasmic reticulum; 3β-HSD, 3β-hydroxysteroid dehydrogenase; 20α-HSD, 20α-hydroxysteroid dehydrogenase.

each estrous stage, and new CL drastically change their morphology and function of P4 secretion during the estrous cycle (Taketa et al. 2011b; Yoshida et al. 2009). Old CL do not have the function of P4 secretion but morphologically can be classified into distinct types at the estrous stage during regression (Taketa et al. 2011b).

In rats, PRL has both luteotrophic and luteolytic actions depending on the stage of the estrous cycle or in the pregnant or pseudopregnant state. During mating, cervical stimulation activates a neuroendocrine reflex of circadian nocturnal PRL surges, which maintain CL and its secretion of P4 (Rehm et al. 2007). Therefore, sustained PRL secretion preserves functional CL. Meanwhile, since preovulatory PRL surge in the rat estrous cycle induces regression of nonfunctional CL, sustained inhibition of PRL secretion prevents luteolysis (Gaytan et al. 2001; Rehm et al. 2007).

We have previously shown that EGME and atrazine, respectively, induces luteal cell hypertrophy and increases P4 secretion in their cells with and without PRL hypersecretion (Taketa et al. 2011a). Furthermore, EGME increased P4 synthesis factor expression both in new and in old CL, whereas atrazine stimulated P4 synthesis factors expression in new CL. These results indicated that EGME stimulates luteal steroidogenesis in both PRL-dependent and PRL-independent manners, while atrazine stimulates luteal steroidogenesis in a PRL-independent manner. Since the molecular biological effect in the CL was different between EGME and atrazine treatments, it suggested that these chemicals may also have different morphological influences on the CL. However, these influences have not yet been examined. Additionally, the luteal histopathological effect of BRC is still not fully understood. The present study describes the detailed morphological characterization of EGME, atrazine, or BRC on the CL by light and electron microscopy. Since BRC is the strong inhibitor of PRL release, this study also examines the PRL-independent morphological luteal effect of EGME under a PRL-inhibitory state by coadministration of EGME and BRC to normal estrous cycling rats.

MATERIALS AND METHODS

Animals

Female 8-week-old Sprague-Dawley (Crl:CD) rats were purchased from Charles River Laboratories Japan, Inc. (Yokohama, Japan). After 2 weeks of acclimation, they were housed in a clean air room maintained at 23°C to 25°C and a relative humidity of 50% to 60% with a 12-hr light cycle. Commercial rodent chow (CRF-1; Oriental Yeast Co., Ltd., Tokyo, Japan) and drinking water were available *ad libitum*. Estrous cycle stage was determined each morning by vaginal smear throughout the experimental period. Only animals displaying 4-day estrous cycles were included in the experiments. The animal protocols were reviewed and approved by the Animal Care and Use Committee of the National Institute of Health Sciences, Japan.

Chemicals and Reagents

EGME, purchased from Wako Pure Chemical Industries, Ltd. (Osaka, Japan), was dissolved in water for injection. Atrazine, purchased from Tokyo Chemical Industry (Tokyo, Japan), was suspended in 0.5 w/v% methyl cellulose 400 solution (Wako Pure Chemical Industries, Ltd.). BRC, purchased from Sigma-Aldrich (St. Louis, MO), was dissolved in 70% ethanol diluted with saline. Control animals received 0.5 w/v% methyl cellulose 400 solution by gavage and 70% ethanol diluted with saline by subcutaneous administration.

Study Design

EGME (300 mg/kg/day) or atrazine (300 mg/kg/day) was administered by gavage and BRC (2 mg/kg/day) was subcutaneously administered to rats once per day for 7 days. For evaluating the effects of EGME on the luteal cells in the absence of PRL, the animals were coadministrated with EGME (300 mg/kg/day, gavage) and BRC (2 mg/kg/day, subcutaneously; EGME + BRC) once per day for 7 days. Effective doses of EGME, atrazine, and BRC were selected based on previous reports (Dodo et al. 2009; Kumazawa et al. 2009; Shibayama et al. 2009; Taketa et al. 2011a). On the morning after the last treatment, the animals were euthanized by decapitation (n = 4–5/group). Considering the estrous cyclicity, the administration to all animals was started at the proestrus stage and the control and BRC-treated animals were euthanized at the diestrus stage after 7-day treatment. Since repeated administration of EGME, EGME + BRC, or atrazine disrupts the estrous cycle, animals in these groups did not synchronize to stage of the estrous cycle at necropsy.

Light Microscopy and Electron Microscopy

For light microscopic examination, unilateral ovary was fixed in 10 vol% neutral-buffered formalin and processed with hematoxylin and eosin (H&E) staining. The number of total CL and two types of hypertrophic CL were counted in two sections of the ovary. The vagina and uterus were also microscopically examined to confirm the estrous stage.

For ultrastructural analysis, contralateral CL was separately removed from the other side of the ovary used above for light microscopy and was fixed in 3% glutaraldehyde in 0.1 M phosphate buffer solution (PBS) for 24 hr. After rinsing in the same buffer, the CL was postfixed in 1% osmium tetroxide (OsO_4) in 0.1 M PBS for 2 hr. The tissue was then dehydrated through a graded series of ethanol and embedded in epon812. One-micron sections were stained with toluidine blue, the CL types (CL-V or CL-E) were distinguished, and selected blocks were thin sectioned. The grids were stained with 1% uranyl acetate for 20 min at room temperature (RT), rinsed 3 times with distilled water (DW), stained with lead citrate (Millonig 1961) for 10 min at RT, rinsed 3 times with DW, and air-dried. The grids were examined with the JEM-1400 Electron Microscope (JEOL Ltd., Tokyo, Japan) and photomicrographs were obtained with an ORIUS CCD camera (Gatan, Inc., Pleasanton, CA).

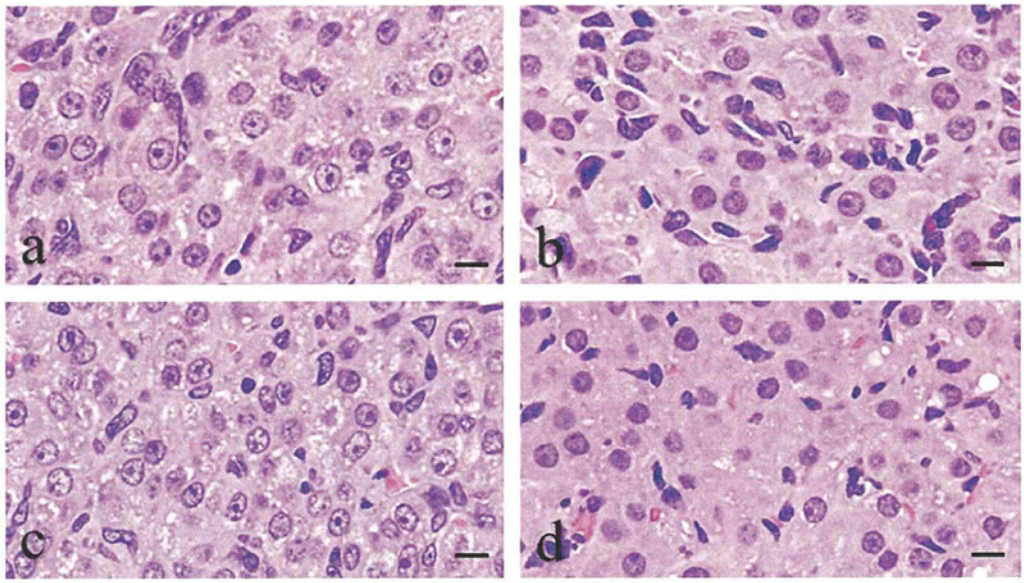

FIGURE 1.—Light microscopic changes in new corpora lutea (CL) (a) and old CL (b) in the control group at the diestrus stage, and CL treated by BRC (c and d) for 7 days. The bromocriptine (BRC)-treated new CL (c) was not different from the control new CL (a) whereas the old CL showed less interstitial cells (d) compared to the control CL (b). H&E staining. Bars represent 10 μm.

RESULTS

Light Microscopic Luteal Changes by EGME, Atrazine, or BRC Treatment

During the diestrus stage, the control group produced luteal cells of the new CL, which exhibited pale eosinophilic staining in the cytoplasm with sparse and fine vacuolation (Figure 1a); while the luteal cells of the old CL exhibited strong eosinophilic staining in the cytoplasm and the additional presence of interstitial cells, such as endothelial cells and fibroblasts (Figure 1b). In the BRC group, the luteal features of the new CL were similar to the control group (Figure 1c). Although all BRC-treated animals represented normal estrous cyclicity and the luteal cell shape and size of the old CL in the BRC group showed no apparent changes compared to the control group, the proportion of interstitial cells in the old CL of the BRC group was lower than that in the old CL of the control group (Figure 1d). In the EGME, EGME + BRC, and atrazine groups, a large number of luteal cells were hypertrophic and the CL were categorized into two types according to the hypertrophic luteal cell types: CL hypertrophy, vacuolated type (CL-V) and CL hypertrophy, eosinophilic type (CL-E). It was hard to distinguish the new CL from the old CL because of the luteal cell hypertrophy. The luteal cells of CL-V contained rich and fine vacuoles in cytoplasm (Figure 2a, c, and e), whereas those of CL-E had eosinophilic and abundant cytoplasm (Figure 2b, d, and f). Furthermore, each luteal cell of both CL types had distinct cell borders. The individual luteal cells of CL-V and CL-E in the EGME + BRC group were more hypertrophic than those in the EGME and atrazine groups (Figure 2). In the EGME and EGME + BRC groups, CL-E were more frequently observed than CL-V, while both CL-V and CL-E were uniformly observed in the atrazine group (Table 1). Interstitial cells in CL-V were sparse, whereas some CL-E contained many interstitial cells in the EGME, EGME + BRC, and atrazine groups.

Ultrastructural Luteal Changes by EGME, Atrazine, or BRC Treatment

There was no obvious luteal ultrastructural difference between new CL and old CL at the diestrus stage in the control group. During the diestrus stage, lipid droplets, smooth and rough endoplasmic reticulum (SER and RER, respectively), and mitochondria were uniformly distributed in the luteal cells of the control group (Figures 3a and 4a). The luteal cells of CL-V in the EGME, EGME + BRC, and atrazine groups contained abundant lipid droplets (Figure 3c-e). Although the large-sized of lipid droplets tended to be observed in the EGME-treated and EGME + BRC-treated luteal cells of CL-V, they were judged to be within normal ranges because of the various sizes of lipid droplets in the control luteal cells (Figure 3a, c, and d). The atrazine-

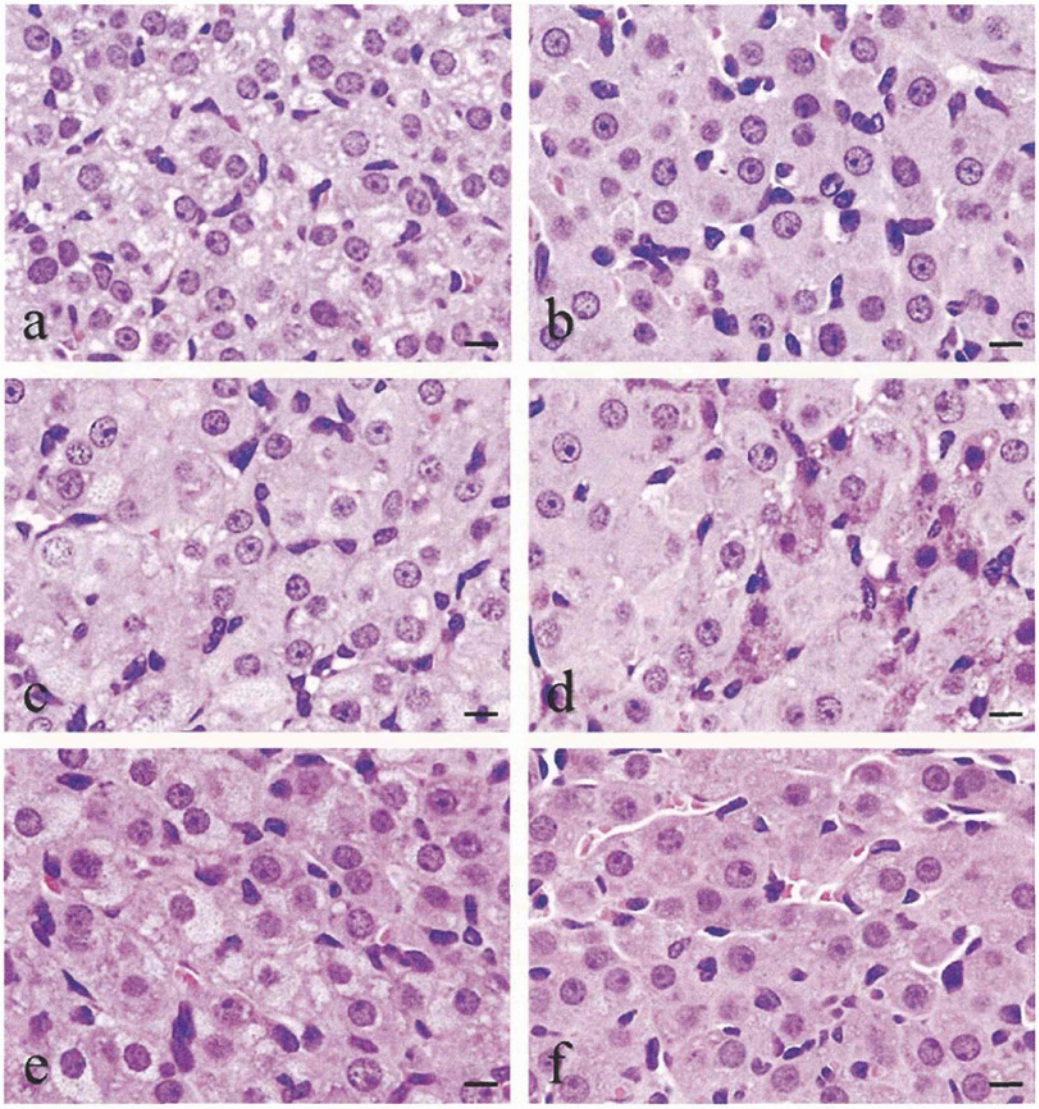

FIGURE 2.—Light microscopic changes in corpora lutea (CL) treated by ethylene glycol monomethyl ether (EGME) (a and b), EGME + bromocriptine (BRC) (c and d), or atrazine (e and f) for 7 days. The hypertrophic luteal cells of CL-V had fine vacuolated cytoplasm by EGME (a), EGME + BRC (c), or atrazine (e) treatment. The hypertrophic luteal cells of CL-E contained eosinophilic and abundant cytoplasm by EGME (B), EGME + BRC (d), or atrazine (f) treatment. H&E staining. Bars represent 10 μm.

treated luteal cells of CL-V showed similar-sized lipid droplets to the control group (Figure 3a and e). The luteal cells of CL-E in the EGME and EGME + BRC groups were characterized by uniformly well-developed SER (Figure 4c and d) and occasional abundant mitochondria. No obvious luteal changes were found in the atrazine-treated CL-E (Figure 4e). The ultrastructure of the luteal cells of the BRC group was similar to the control group (Figures 3a, b and 4a, b).

TABLE 1.—Number and percentage of CL-V and CL-E in total CL

Treatment	Vehicle	BRC	EGME	EGME + BRC	Atrazine
Number of CL-V	–	–	1.3 ± 1.3	7.3 ± 1.3	7.7 ± 1.5
Number of CL-E	–	–	11.7 ± 3.3	18.8 ± 2.1	9.3 ± 1.2
Total CL number	37.0 ± 5.6	39.0 ± 4.9	36.7 ± 3.5	43.3 ± 4.8	41.0 ± 2.3
Percentage of CL-V	–	–	4.3 ± 4.3	16.5 ± 1.5	18.7 ± 3.2
Percentage of CL-E	–	–	30.9 ± 7.6	43.5 ± 2.4	22.8 ± 3.0

Values are presented as the mean ± *SEM* (*n* = 3–4/group). The number of CL was counted in two sections of the ovary. – = not applicable; BRC = bromocriptine; EGME = ethylene glycol monomethyl ether; CL-V = corpora lutea, vacuolated type; CL-E = corpora lutea, eosinophilic type. *SEM* = standard error of the mean.

DISCUSSION

This study focused on light- and electron-microscopic changes of the luteal cells induced by EGME, atrazine, or BRC in rats. A large number of CL representing luteal cell hypertrophy by 7 days of treatment with EGME or atrazine indicate that EGME and atrazine affect both new and old CL. This change was also observed by coadministration of EGME and BRC, indicating that EGME morphologically affects luteal cells without PRL release. Considering our previous study that the concurrent administration of EGME with BRC stimulated P4 secretion, upregulated steroidogenic factor expression levels, and downregulated luteolytic factor expression levels in luteal cells without PRL hypersecretion (Taketa et al. 2011a), the main luteal stimulatory effect of EGME seems to be independent of PRL. In the EGME, EGME + BRC, and atrazine groups, the CL hypertrophy was classified into two types by light microscopy, CL-V and CL-E. The proportions of CL-V and CL-E were different among the treatment groups, suggesting that chemically induced luteal hypertrophy does not mean similar morphology. Although the low proportion of interstitial cells in the BRC-treated old CL indicates that BRC treatment inhibited regression of old CL, their luteal cells were not hypertrophic. This change was presumably caused by the inhibition of the PRL surge that initiates structural luteolysis in rats, by the D2 agonistic effect (Gaytan et al. 2001). Since the animals had passed only one complete estrous cycle during the administration, the increase in CL number by BRC treatment was not obvious. The increase in the number and size of CL-V and CL-E by the EGME + BRC treatment in comparison to the EGME-only treatment was considered to be due to the luteolysis inhibitory effect of BRC.

Electron microscopic observation revealed that luteal hypertrophy of CL-V in the EGME, EGME + BRC, and atrazine groups was caused by excessive storage of lipid droplets. On the contrary, luteal hypertrophy of CL-E in the EGME and EGME + BRC groups resulted from excessive SER development. Occasional increase in mitochondria suggested the possibility that EGME may also affect mitochondrial function and development in CL-E. In the pregnant rats, luteal cells became enlarged and the amount of SER greatly increased by 7 to 10 days of pregnancy (Long 1973). Since the increase in PRL secretion is observed in the first 10 days of pregnancy (Egli et al. 2010), PRL seems to enhance SER development in the new CL. Considering the same luteal change in the EGME + BRC-treated CL-E, EGME may also stimulate luteal SER development in a PRL-independent manner. The CL reached a maximum size and had maximal P4 secretory activity at approximately 16 to 17 days of pregnancy, and the luteal cells exhibited strong proliferation of SER membranes (Long 1973; Meyer and Bruce 1984). These reports indicate that luteal cell hypertrophy in the functional CL is typically due to the development of SER. Therefore, EGME-induced CL-E, which contained well-developed SER, support sufficient P4 secretory function. On the other hand, lipid accumulation in the CL was seen only in early pregnancy in rats (Long 1973). These observations indicate a possibility that luteal morphology might be altered by the duration of the stimulatory period. That is, short-term or intermittent stimulation may result in lipid accumulation to uptake the source of cholesterol, whereas long-term or continuous stimulation seems to induce SER development for the activation of P4 synthesis in the luteal cells. It was previously shown that glucocorticoids stimulated the accumulation of lipid droplets and steroidogenesis with increased 20α-hydroxysteroid dehydrogenase (20α-HSD) secretion in rat CL (Towns et al. 1999). This previous report and the present study suggest that CL-V also have the capacity for steroid synthesis though their P4 secretion capacity may be lower than CL-E due to the increase in 20α-HSD.

The origin of CL-V and CL-E is still not fully understood. From our previous study, EGME elicited luteal changes in both the new and old CL, with the new CL being the principal target (Taketa et al. 2011a). Given the possibility of high P4 synthesis capacity in CL-E, the CL-E may have originated from the new CL in EGME-treated and EGME + BRC-treated CL. However, light microscopic changes revealed many interstitial cells in several CL-E, indicating that some CL-E may have been from the old CL. The scarce interstitial cells in CL-V suggest that the new CL seem to be the origin of EGME-treated and EGME + BRC-treated CL-V. We have already shown the increase in 3β-hydroxysteroid dehydrogenase (3β-HSD) expression in the old CL by EGME treatment (Taketa et al. 2011a). Since 3β-HSD localizes in the SER (Stocco et al. 2007), it is probable that some of the CL-E, which contains abundant SER, originated from old CL in the EGME and EGME + BRC groups.

Considering the scarce interstitial cells and high proportion of atrazine-treated CL-V in the present study and new CL was the main stimulatory target of atrazine in our previous study (Taketa et al. 2011a), atrazine-treated CL-V was assumed to be derived

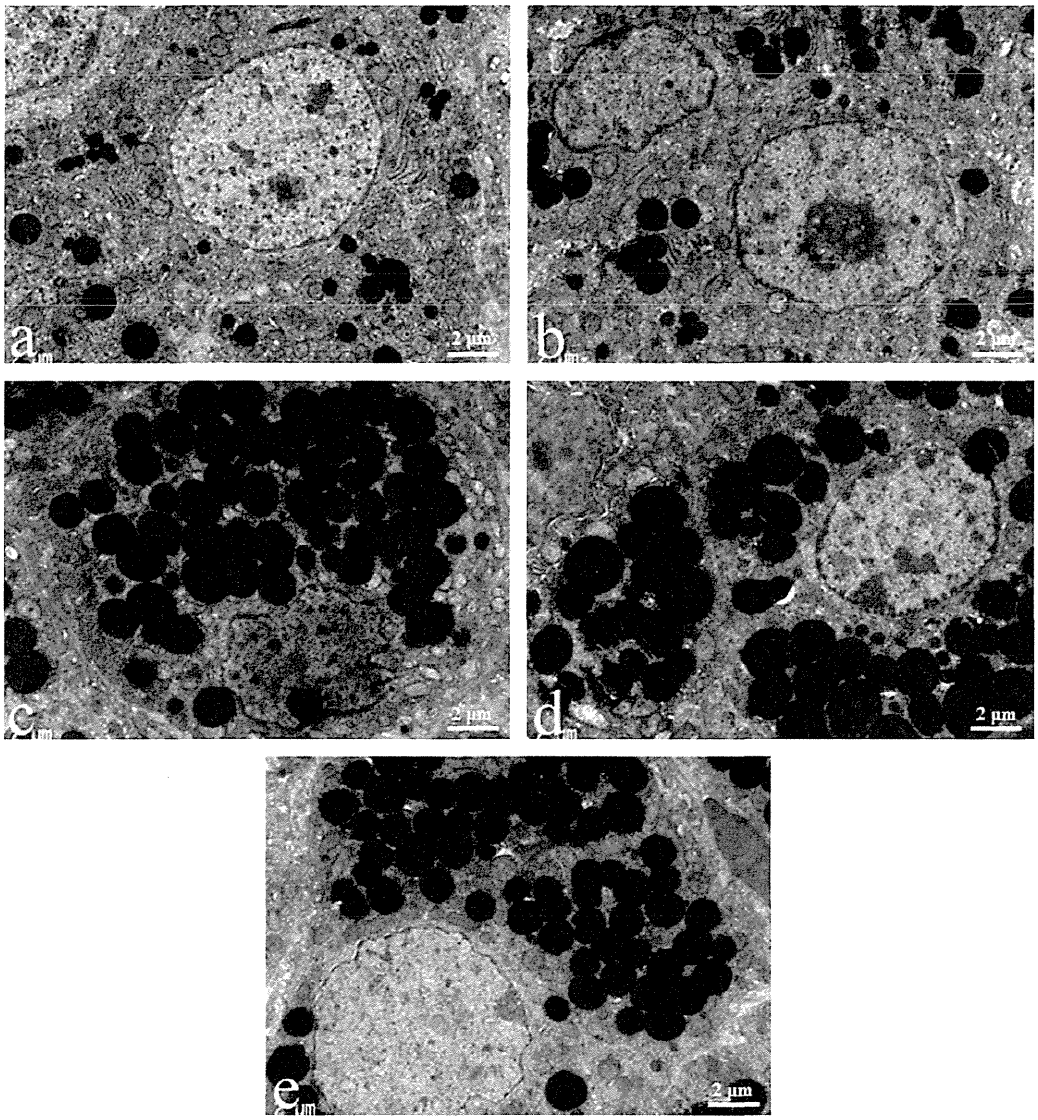

FIGURE 3.—Ultrastructural luteal changes induced by treatment with bromocriptine (BRC), ethylene glycol monomethyl ether (EGME), EGME + BRC, or atrazine. The hypertrophic luteal cells of corpora lutea, vacuolated type (CL-V) contained abundant lipid droplets following EGME (c), EGME + BRC (d), or atrazine (e) treatment compared to the control new CL at the diestrus stage (a). BRC-treated new CL (b) was not different from the control new CL. Magnification 8,000×.

from new CL. This observation suggests that atrazine stimulates the accumulation of lipid droplets in the new CL. It is still unclear why atrazine-treated CL-E became hypertrophic without apparent ultrastructural change. One possibility is that the atrazine-treated CL-E was not functionally activated. Since atrazine did not stimulate old CL in our previous study, the

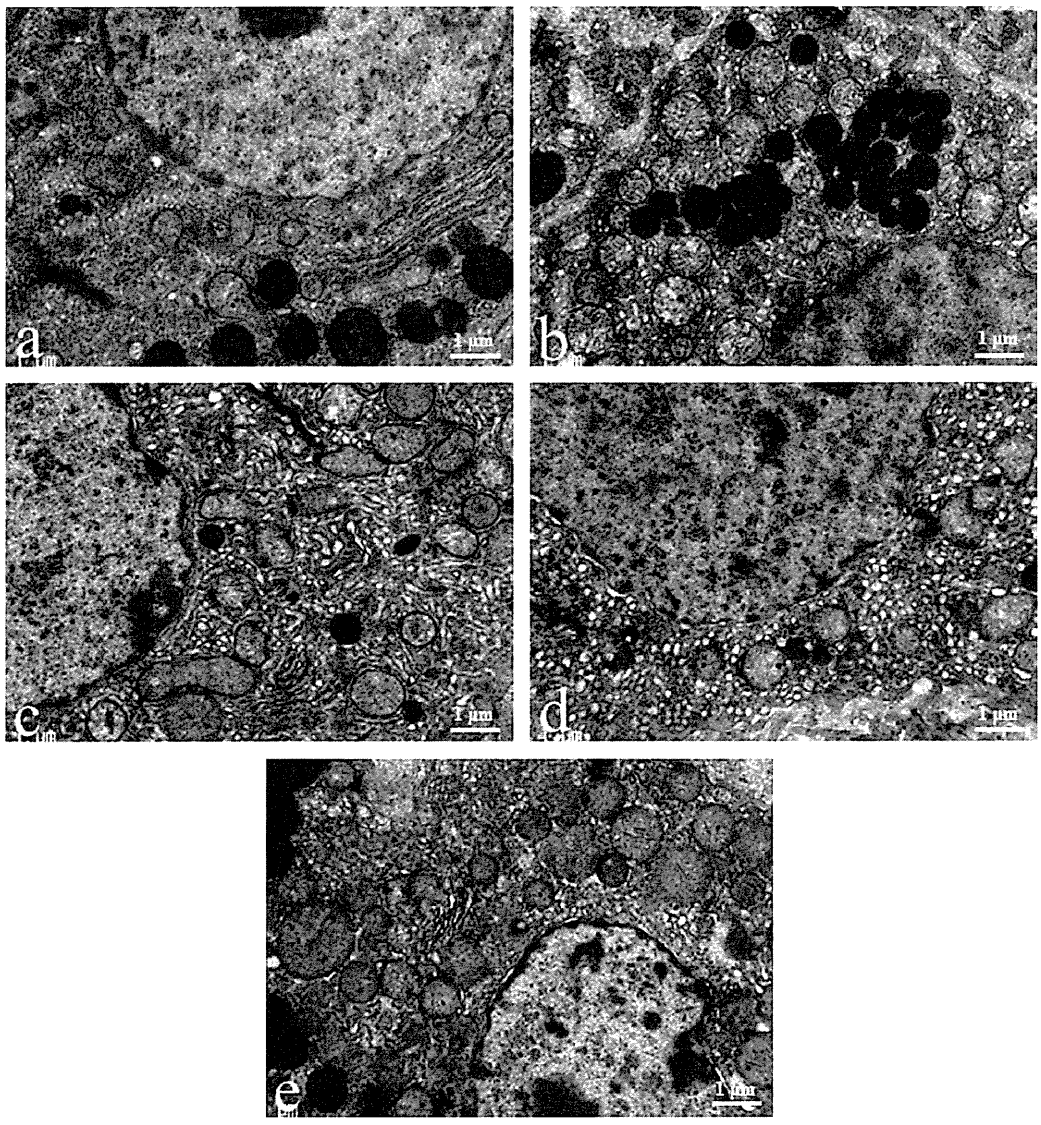

FIGURE 4.—Ultrastructural luteal changes induced by treatment with bromocriptine (BRC), ethylene glycol monomethyl ether (EGME), EGME + BRC, or atrazine. The hypertrophic luteal cells of corpora lutea, eosinophilic type (CL-E) contained well-developed smooth endoplasmic reticulum following EGME (c) or EGME + BRC (d) treatment compared to the control new CL at the diestrus stage (a). BRC-treated new CL (b) or atrazine-treated CL-E (e) was not obviously different from the control new CL. Magnification ×15,000.

atrazine-induced CL-E in the present study might be derived from old CL (Taketa et al. 2011a). The further morphological investigations about atrazine-induced CL-E are required.

In our previous study, EGME induced luteal hypertrophy at higher than 100 mg/kg/day (Taketa et al. 2010). Similarly, *in vitro*, EGME stimulates P4 secretion at concentrations more

than 100 mg/kg in human and rat luteal cells (Almekinder et al. 1997; Davis et al. 1997). From these data, a similar affect level of EGME in luteal cells between human and rat could be predicted. The luteal toxicity of atrazine in human has been undetermined. Although the affecting dose level of 300 mg/kg/day in this study seems to be quite high compared to the human exposure level of atrazine reported in United States (1.8–6.1 μg/kg/day; Gammon et al. 2005), its potency of luteal toxicity should be noted. Further investigations about luteal toxicity of EGME and atrazine in humans are required.

In conclusion, the morphological differences of CL-V and CL-E in response to EGME and atrazine treatment reflect a distinct capacity of each CL type for steroidogenesis. However, the present study is a short-term investigation of luteal toxicity in response to EGME and atrazine; therefore, further studies investigating the long-term morphological effects are required.

ACKNOWLEDGMENTS

We thank Ms. Tomomi Morikawa, Ms. Ayako Kaneko, and Ms. Yoshimi Komatsu for their excellent technical assistance. We also appreciate Dr. Satoru Hosokawa and Dr. Akira Inomata (Drug Safety Japan, Global Drug Safety, Biopharmaceutical Assessments Core Function Unit, Eisai Product Creation Systems, Eisai Co., Ltd.) for their helpful suggestions.

REFERENCES

Almekinder, J. L., Lennard, D. E., Walme, D. K, and Davi, B. J. (1997). Toxicity of methoxyacetic acid in cultured human luteal cells. *Fundam Appl Toxicol* **38**, 191–94.

Bowen, J. M., and Keyes, P. L. (2000). Repeated exposure to prolactin is required to induce luteal regression in the hypophysectomized rat. *Biol Reprod* **63**, 1179–84.

Cooper, R. L., Stoker, T. E., Tyrey, L., Goldman, J. M., and McElroy, W. K. (2000). Atrazine disrupts the hypothalamic control of pituitary-ovarian function. *Toxicol Sci* **53**, 297–307.

Davis, B. J., Almekinder, J. L., Flagler, N., Travlos, G., Wilson, R., and Maronpot, R. R. (1997). Ovarian luteal cell toxicity of ethylene glycol monomethyl ether and methoxy acetic acid in vivo and in vitro. *Toxicol Appl Pharmacol* **142**, 328–37.

Dodo, T., Taketa, Y., Sugiyama, M., Inomata, A., Sonoda, J., Okuda, Y., Mineshima, H., Hosokawa, S., and Aoki, T. (2009). Collaborative work on evaluation of ovarian toxicity. 11) Two- or four-week repeated-dose studies and fertility study of ethylene glycol monomethyl ether in female rats. *J Toxicol Sci* **34**, SP121–28.

Egli, M., Leeners, B., and Kruger, T. H. (2010). Prolactin secretion patterns: Basic mechanisms and clinical implications for reproduction. *Reproduction* **140**, 643–54.

Eldridge, J. C., Tennant, M. K., Wetzel, L. T., Breckenridge, C. B., and Stevens, J. T. (1994). Factors affecting mammary tumor incidence in chlorotriazine-treated female rats: hormonal properties, dosage, and animal strain. *Environ Health Perspect* **102**, 29–36.

Eldridge, J. C., Wetzel, L. T., and Tyrey, L. (1999). Estrous cycle patterns of Sprague- Dawley rats during acute and chronic atrazine administration. *Reprod Toxicol* **12**, 491–99.

Foradori, C. D., Hinds, L. R., Hanneman, W. H., Legare, M. E., Clay, C. M., and Handa, R. J. (2009). Atrazine inhibits pulsatile luteinizing hormone release without altering pituitary sensitivity to a gonadotropin-releasing hormone receptor agonist in female Wistar rats. *Biol Reprod* **81**, 40–45.

Fraites, M. J., Cooper, R. L., Buckalew, A., Jayaraman, S., Mills, L., and Laws, S. C. (2009). Characterization of the hypothalamic-pituitary-adrenal axis response to atrazine and metabolites in the female rat. *Toxicol Sci* **112**, 88–99.

Gammon, D. W., Aldous, C. N., Carr, W. C. Jr., Sanborn, J. R., and Pfeifer, K. F. (2005). A risk assessment of atrazine use in California: Human health and ecological aspects. *Pest Manag Sci* **61**, 331–55.

Gaytan, F., Bellido, C., Morales, C., and Sanchez-Criado, J. E. (2001). Luteolytic effect of prolactin is dependent on the degree of differentiation of luteal cells in the rat. *Biol Reprod* **65**, 433–41.

Johanson, G. (2000). Toxicity review of ethylene glycol monomethyl ether and its acetate ester. *Crit Rev Toxicol* **30**, 307–45.

Kumazawa, T., Nakajima, A., Ishiguro, T., Jiuxin, Z., Tanaharu, T., Nishitani, H., Inoue, Y., Harada, S., Hayasaka, I., and Tagawa, Y. (2009). Collaborative work on evaluation of ovarian toxicity. 15) Two- or four-week repeated-dose studies and fertility study of bromocriptine in female rats. *J Toxicol Sci* **34**, SP157–65.

Long, J. A. (1973). Corpus luteum of pregnancy in the rat–ultrastructural and cytochemical observations. *Biol Reprod* **8**, 87–99.

Meyer, G. T., and Bruce, N. W. (1984). Quantitative ultrastructure of the luteal cell of the 16-day-pregnant rat and its relation to progesterone secretion. *J Reprod Fertil* **70**, 261–69.

Millonig, G. (1961). A modified procedure for lead staining of thin sections. *J Biophys Biochem Cytol* **11**, 736–39.

Rehm, S., Stanislaus, D. J., and Wier, P. J. (2007). Identification of drug-induced hyper- or hypoprolactinemia in the female rat based on general and reproductive toxicity study parameters. *Birth Defects Res B Dev Reprod Toxicol* **80**, 253–57.

Sanbuissho, A., Yoshida, M., Hisada, S., Sagami, F., Kudo, S., Kumazawa, T., Ube, M., Komatsu, S., and Ohno, Y. (2009). Collaborative work on evaluation of ovarian toxicity by repeated-dose and fertility studies in female rats. *J Toxicol Sci* **34**, SP1–22.

Shibayama, H., Kotera, T., Shinoda, Y., Hanada, T., Kajihara, T., Ueda, M., Tamura, H., Ishibashi, S., and Yamashita, Y. (2009). Collaborative work on evaluation of ovarian toxicity. 14) Two- or four-week repeated-dose studies and fertility study of atrazine in female rats. *J Toxicol Sci* **34**, SP147–55.

Stocco, C., Telleria, C., and Gibori, G. (2007). The molecular control of corpus luteum formation, function, and regression. *Endocr Rev* **28**, 117–49.

Stouffer, R. L. (2006). Structure, function, and regulation of the corpus luteum. In *Knobil and Neill's Physiology of Reproduction* (J. D. Neill, ed.), 3rd ed., pp. 475–526. Elsevier Academic Press, San Diego, CA.

Taketa, Y., Inomata, A., Hosokawa, S., Sonoda, J., Hayakawa, K., Nakano, K., Momozawa, Y., Yamate, J., Yoshida, M., Aoki, T., and Tsukidate, K. (2010). Histopathological characteristics of luteal hypertrophy induced by ethylene glycol monomethyl ether with a comparison to normal luteal morphology in rats. *Toxicol Pathol* **39**, 372–80.

Taketa, Y., Yoshida, M., Inoue, K., Takahashi, M., Sakamoto, Y., Watanabe, G., Taya, K., Yamate, J., and Nishikawa, A. (2011a). Differential stimulation pathways of progesterone secretion from newly formed corpora lutea in rats treated with ethylene glycol monomethyl ether, sulpiride, or atrazine. *Toxicol Sci* **121**, 267–78.

Taketa, Y., Yoshida, M., Inoue, K., Takahashi, M., Sakamoto, Y., Watanabe, G., Taya, K., Yamate, J., and Nishikawa, A. (2011b). The newly formed corpora lutea of normal cycling rats exhibit drastic changes in steroidogenic and luteolytic gene expressions. *Exp Toxicol Pathol* doi: 10.1016/j.etp.2011.01.015. [Epub ahead of print].

Tinfo, N. S., Hotchkiss, M. G., Buckalew, A. R., Zorrilla, L. M., Cooper, R. L., and Laws, S. C. (2011). Understanding the effects of atrazine on steroidogenesis in rat granulosa and H295R adrenal cortical carcinoma cells. *Reprod Toxicol* **31**, 184–93.

Towns, R., Menon, K. M., Brabec, R. K., Silverstein, A. M., Cohen, J. M., Bowen, J. M., and Keyes, P. L. (1999). Glucocorticoids stimulate the accumulation of lipids in the rat corpus luteum. *Biol Reprod* **61**, 416–21.

Welsch, F. (2005). The mechanism of ethylene glycol ether reproductive and developmental toxicity and evidence for adverse effects in humans. *Toxicol Lett* **156**, 13–28.

Yoshida, M., Sanbuissyo, A., Hisada, S., Takahashi, M., Ohno, Y., and Nishikawa, A. (2009). Morphological characterization of the ovary under normal cycling in rats and its viewpoints of ovarian toxicity detection. *J Toxicol Sci* **34**, SP189–97.

Yuan, Y., and Foley, G. L. (2002). Female reproductive system. In Handbook of Toxicologic Pathology (W. M. Haschek, C. G. Rousseaux, and M. S. Wallig, eds.), **Vol. 2**, pp. 847–94. Academic Press, London, UK.

Exp. Anim. 61(5), 517–524, 2012

—Original—

Male Hatano High-Avoidance Rats Show High Avoidance and High Anxiety-Like Behaviors as Compared with Male Low-Avoidance Rats

Yasuyuki HORII[1,2], Maiko KAWAGUCHI[3,4], Ryo OHTA[5], Akihiro HIRANO[3,4], Gen WATANABE[1,2], Nobumasa KATO[6,7], Toshiyuki HIMI[4] and Kazuyoshi TAYA[1,2]

[1]*Department of Basic Veterinary Science, United Graduate School of Veterinary Sciences, Gifu University, 1–1 Yanagido, Gifu, Gifu 501-1193, Japan*
[2]*Laboratory of Veterinary Physiology, Tokyo University of Agriculture and Technology, 3–5–8 Saiwaicho, Fuchu, Tokyo 183-8509, Japan*
[3]*School of Agriculture, Meiji University, 1–1–1 Higashimita, Tama-ku, Kawasaki, Kanagawa 214-8571, Japan*
[4]*Faculty of Pharmacy and Research Institute of Pharmaceutical Science, Musashino University, 1–1–20 Shinmachi, Nishi-Tokyo, Tokyo 202-8585, Japan*
[5]*Division of Toxicology, Hatano Research Institute, Food and Drug Safety Center, 729–5 Ochiai, Hadano, Kanagawa 257-8523, Japan*
[6]*Department of Psychiatry, Showa University School of Medicine, 6–11–11 Kita-Karasuyama, Setagaya-ku, Tokyo 157-8577, Japan*
[7]*JST, CREST*

Abstract: Our prime objective was to establish an optimal model animal for studying avoidance learning and memory in rodents. The two-way rat inbred strains of Hatano high- (HAA) and low-avoidance (LAA) animals were originally selected and bred in accordance with their high or low performance respectively in the shuttle-box active avoidance task. Previous studies demonstrated that they have clear strain differences in endocrine stress response, which is related to acquisition of aversive learning and emotional reactivity. To evaluate the effect of selection by the shuttle-box task on avoidance performance and emotional reactivity, male Hatano rats underwent passive avoidance, open field and elevated plus maze tests. The present results show that the avoidance performance in the passive task was significantly greater in HAA rats than in LAA rats. Furthermore, HAA rats showed high anxiety-like behaviors compared with LAA rats in open field and elevated plus maze tests. Taken together, this study demonstrated that 1) selection and breeding of Hatano HAA and LAA strain rats by shuttle-box task had been properly carried out with the criterion of high and low avoidance performance respectively and that 2) HAA rats were predisposed to high anxiety compared with LAA rats. These results indicated that Hatano HAA and LAA rats can be useful models for studying avoidance learning and memory.

Key words: anxiety, elevated plus maze test, hatano rats, learning and memory, passive avoidance task

Introduction

The prime objective in the present study was to establish an optimal model for studying avoidance learning and memory in rodents. For a prey like the rodents, understanding and avoiding aversive situations is very essential to their survival and to conserve the species. Thus, emotionality, especially anxiety and fearfulness, could be an important factor in exhibiting defensive reactions and learning and memorizing aversive situations [14].

(Received 12 March 2012 / Accepted 8 May 2012)

Address corresponding: M. Kawaguchi, School of Agriculture, Meiji University, 1–1–1 Higashimita, Tama-ku, Kawasaki, Kanagawa 214-8571, Japan

Animals have their own species-specific defensive reactions (SSDRs) in nature, such as escape, freezing, attacking and defensive burying behaviors in rats [14]. In the laboratory, there are 2 major behavioral paradigms of avoidance learning tasks in rats, such as active and passive avoidance tasks [22, 30]. For the shuttle-box active avoidance task [30], an animal is first given light and buzzer alarms as condition stimuli (CS) and continuously given foot shocks as unconditioned stimuli (US). Animals that have learned about the CS begin to flee to an adjacent non-stress chamber before they receive US or begin to freeze in place without US, but animals that have not learned about CS flee to the non-stress chamber after receiving US or begin to freeze in place with US. Thus, freezing rats might show low avoidance rates regardless of CS learning in the active task. For the step-through type passive avoidance task [22], the apparatus consisted of 2 chambers, light and dark boxes. Once an animal is placed in the light box, it quickly moves to dark box because rodents prefer darker places in nature. In the dark box, the animal is given an unavoidable foot shock as a learning session. After few minutes, 24 h, several days or more, the same procedure is repeated and the latency in entering the dark box is recorded as memory retention. As moving or staying allows the animal to avoid US, it is called an active or passive avoidance task, respectively.

Hatano high- (HAA) and low-avoidance (LAA) animals that were derived from Sprague-Dawley (SD) rats (Charles River Laboratories Japan, Inc., Kanagawa, Japan) were selectively bred on the basis of high or low avoidance rates respectively in the shuttle-box active avoidance task [30]. For the selection of Hatano rats, 48 SD rats (24 males and 24 females) were used as the first parental population. The male and female SD rats showing the highest or lowest avoidance responses during 4 daily sessions of 60 trials were selected and mated with each other as HAA or LAA, respectively. For LAA, noteworthy animals showing freezing behavior were removed at every generation [31] because it might be included CS learning animal but showing low avoidance performance as mentioned above. Selection by shuttle-box task was similarly applied for more than 20 generations, and HAA and LAA were maintained through full sib-mating for more than 60 generations since 1985. Remarkably, the avoidance response in the shuttle-box task might not be only due to the CS learning but might also be due to the cumulative effect of other factors such as locomotor activity, emotionality and response to stress [7, 10–12, 35]. Indeed, some other shuttle-box two-way selective inbred rats showed a discrepancy in the results of the passive avoidance paradigm [8–10, 15, 16]. Thus, testing avoidance performance in a manner other than the shuttle-box task is also required to firmly demonstrate the utility of Hatano rats in studying avoidance learning and memory. Moreover, our previous reports demonstrated that HAA and LAA have strain differences in locomotor activity and endocrine stress response [2–4, 21, 28, 31]. In brief, HAA shows high activity in running wheel cage [28], high adrenocorticotropin (ACTH) and low prolactin in plasma during restraint stress compared with LAA [2, 4]. But emotional characteristics of Hatano rats have not been investigated yet.

Furthermore, it is known that the performance of passive avoidance is higher in adolescents (180 days old) or adults (365 days old) than in juveniles (30 days old) or old rats (547 days old) [27]; also, juvenile male rats show high and well-rounded activity in open field and elevated plus maze tests, respectively, as compared with the other developmental stages [19, 26]. Thus, in the present study, adolescent and juvenile male Hatano rats were investigated for their avoidance learning by passive avoidance task and for anxiety-like behaviors by open field and elevated plus maze tests, respectively, to evaluate the effects of selection by the shuttle-box task on avoidance performance and emotional reactivity.

Materials and Methods

Animals

HAA rats from the 62nd generation and LAA rats from the 60th generation produced at Hatano Research Institute were used in the present study. The animals were transported to Musashino University after weaning and kept under standard ambient lighting (0700–1900 h), room temperature (22.5 ± 0.5°C) and humidity conditions (55 ± 10%) and had *ad libitum* access to food (CE2, CLEA Japan, Inc., Tokyo, Japan) and water. All behavioral tests were performed during 0900 to 1600 h, and the same animals were used for all behavioral tests. All experimental procedures used in this study were in accordance with the guidelines of the Animal Care and Use Committee of Musashino University and the Hatano Research Institute of the Food and Drug Safety Center.